



Wavelength-tunable L-band mode-locked fiber laser using a long-period fiber grating

JUNJIE JIANG,¹ QIANQIAN HUANG,¹ YUEHUI MA,¹ DANDAN LIAO,¹
ZINAN HUANG,¹ LILONG DAI,¹ YUNQI LIU,¹  CHENGBO MOU,^{1,*} 
MOHAMMED AL ARAIMI,² AND ALEKSEY ROZHIN^{3,4}

¹Key Laboratory of Specialty Fiber Optics and Optical Access Networks, Shanghai Institute for Advanced Communication and Data Science, Joint International Research Laboratory of Specialty Fiber Optics and Advanced Communication, Shanghai University, Shanghai, 200444, China

²Higher College of Technology, Al-Khuwair, PO Box 74, Postal Code 133, Oman

³Aston Institute of Photonic Technologies, Aston University, Birmingham, B4 7ET, United Kingdom

⁴Nanoscience Research Group, Aston University, Birmingham, B4 7ET, United Kingdom

*mouc1@shu.edu.cn

Abstract: We demonstrate an L-band wavelength-tunable passively mode-locked fiber laser using a single long-period fiber grating (LPFG) as a narrow-band optical attenuator (NBOA). Through bending the LPFG, the central wavelength can be continuously tuned from 1582.02 to 1597.29 nm, while the output power only varies from 1.465 to 1.057 mW, approximately a rate of 22 μ W/nm variation. This is the first time that LPFG is functioned as a NBOA in mode-locked fiber lasers, showing the great advantage of less impact on output power variation reduction. Besides, the total cavity length is 5.08 m, which is the shortest length yet reported in wavelength-tunable mode-locked fiber lasers. The wavelength tuning could also be realized at harmonic mode locking with tuning range of 14.69 nm under 5th harmonic.

© 2021 Optical Society of America under the terms of the [OSA Open Access Publishing Agreement](#)

1. Introduction

Wavelength-tunable mode-locked fiber lasers have been widely used in many fields, such as sensing [1], spectroscopy analysis [2], biomedical research [3], material processing [4,5], optical communication networks [6–9], *etc.* In particular, in some specific applications, for example, dense-wavelength-division-multiplexing systems, the traditional C-band (1530-1565 nm) is not enough to meet the current bandwidth requirements. To enlarge the capacity of the communication system, researchers expand the telecommunications window to L-band (1565-1625 nm) where the loss of silica fiber is low. Therefore, it is necessary to investigate L-band wavelength-tunable mode-locked fiber lasers.

To realize wavelength tuning, one straightforward way is to incorporate a tunable spectral filter in the mode-locked fiber laser cavity. Commercial tunable band-pass filter (CTBPF) [10], chirped fiber Bragg grating (CFBG) [11], long-period fiber grating (LPFG) based W-shaped filter [12], phase shifted LPFG [13], and intracavity birefringence comb filter [14] have been demonstrated successfully in achieving wavelength-tunable mode-locked fiber lasers. An alternative approach to realize wavelength tuning in mode-locked fiber lasers is to control the cavity loss, from which the population inversion levels can be manipulated and the gain profile can be modulated [15]. Lin *et al.* have demonstrated a L-band wavelength-tunable actively mode-locked fiber laser by controlling the output ratio of the coupler to change the cavity loss [16]. Besides, standard variable optical attenuators (VOAs) such as mechanical attenuator (MA) and fiber taper also could be used to control the cavity loss. Zhu *et al.* have realized a wavelength-tunable mode-locked fiber laser covering C + L band based on a MA [17]. Melo *et al.* have realized a L-band wavelength-tunable continuous wave (CW) fiber laser through the loss modulation induced by bending fiber taper [18]. However, the conventional methods of controlling cavity

loss have a great influence on output power since such effect covers the whole effective cavity gain, which may destroy stable mode locking operation. In addition, these methods are usually applied in the lasers with long cavity length, because the insertion of excessive loss would reduce the nonlinearity.

Different from conventional VOAs, a single LPFG can function as a narrow-band optical attenuator (NBOA) in wavelength-tunable fiber lasers (TFLs). The LPFG-type NBOA has great advantages over the traditional VOAs in terms of the stability of output power and laser cavity length since it only suppresses the gain inside its rejection band [19]. This is a well-known effect in a fiber amplifier because the gain equalization can be easily implemented. However, in a fiber laser cavity, such gain equalization (or more precisely gain spectrum control) would induce significant gain drop in a LPFG defined spectral region. Lasing will therefore occur at a broad range within the non-attenuated gain window. Coupled with LPFG's features of robust structure, easy fabrication and low cost, the LPFG-type NBOA becomes a sought-after loss control device in TFLs. Previous studies on LPFG based NBOA in TFLs, those fiber lasers all operated in CW regime [19–22]. Considering the inherent merits of LPFG and the practical applications of wavelength-tunable mode-locked fiber lasers, it is interesting to explore the mode-locked wavelength-tunable fiber lasers using LPFG based NBOA.

In this paper, we realize an L-band wavelength-tunable mode-locked fiber laser using LPFG as a NBOA. By mechanically bending the LPFG, the central wavelength can be continuously tuned from 1582.02 to 1597.29 nm (a total of 15.27 nm) while the output power varies from 1.465 to 1.057 mW, approximately a rate of 22 $\mu\text{W}/\text{nm}$ variation. To the best of our knowledge, this is the first time that LPFG is served as a NBOA in wavelength-tunable mode-locked fiber laser with the low output power variation than those in Ref. [17,23]. In addition, the fundamental repetition rate of output pulse is 41.02 MHz, which is the shorted wavelength tunable mode-locked fiber laser cavity. By increasing pump power and adjusting polarization controller (PC), the wavelength tuning operation can also be achieved at harmonic mode locking. The highest repetition rate of 210.3 MHz, corresponding to the 5th harmonic, is achieved with the associated tuning range of 14.69 nm. The whole tuning process is continuous, controllable, and reversible.

2. Characterization of LPFG and experimental setup

The LPFG, which is designed for operating in L-band, is fabricated in single-mode fiber (SMF) (Corning-28e) where the grating has a period of 410 μm and the number of periods is 90 with the total length of 36.90 mm. The coupling wavelength is dependent of the period of grating Λ and the mode indices of core n_{core} and cladding $n_{clad}^{(m)}$, respectively, where m represents the m th cladding mode, which can be represented by phase-matching condition [24,25]. Therefore, the relative magnitude changes induced in core and cladding mode indices cause the coupling wavelength shift. As we all know, bending LPFG is one of the ways to change the mode indices of core and cladding [24]. Generally, the degree to which the LPFG is bent can be characterized by *curvature*. Figure 1 shows a schematic diagram of calculating curvature. The expression of curvature is as follows:

$$R = (a^2 + h^2)/2h$$

The schematic configuration of the fiber laser is shown in Fig. 1. A section of highly doped erbium fiber (Liekki Er80-8/125) is served as the gain medium, pumped by a 980 nm laser diode via a wavelength division multiplexer (WDM). After that, a single SMF-based LPFG acts as a NBOA. The LPFG is fixed on two translational stages with optical fiber clamps, as shown in Fig. 1. Under the condition of fixed stage 1, the LPFG can be bent by tuning micrometer 2 of 10 μm precision to promote stage 2 move along the horizontal direction. Besides, in order to ensure the unidirectional transmission of signal light in the cavity, a polarization-independent isolator (PI-ISO) is inserted. In addition, a 30:70 coupler extracts 30% of the light outside for

signal detection. To realize self-starting mode locking, a piece of single-walled carbon nanotubes (SWCNTs) film is placed between two fiber connectors. A polarization controller (PC) is used to control the polarization state in the cavity. The whole cavity is 5.08 m including 3.28 m SMF and 1.8 m highly doped erbium fiber (EDF) with the group velocity dispersion of $-22.8 \text{ ps}^2/\text{km}$ and $-20 \text{ ps}^2/\text{km}$, respectively. It is worth mentioning that the length of the EDF used in the cavity is chosen deliberately to work in L-band. The net dispersion of the cavity is -0.11 ps^2 , indicating that the fiber laser operates in soliton regime.

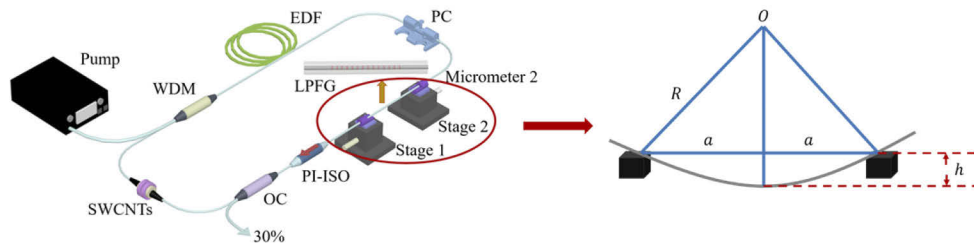


Fig. 1. The schematic diagram of L-band wavelength-tunable passively mode-locked fiber laser based on LPFG.

The optical spectrum is detected by an optical spectrum analyzer (OSA, Yokogawa AQ6370C) with a resolution of 0.02 nm. The characteristics of the output pulse are measured by a 12.5 GHz high speed photo-detector (PD, Newport 818-BB-51F) connected to an 8 GHz oscilloscope (OSC, KEYSIGHT DSO90804A) and a radio frequency (RF) spectrum analyzer (SIGLENT, SSA3032X). Meanwhile, the pulse duration is measured by a commercial autocorrelator (FEMTOCHROME, FR-103XL).

3. Experimental results and discussion

When the pump power reaches 266.1 mW, stable self-started mode locking pulses can be generated and the pulse spectrum is shown in Fig. 2(a), where the central wavelength and 3dB bandwidth are 1582.02 nm and 7.6 nm, respectively. Besides, typical Kelly sidebands demonstrate that the laser operates in the conventional soliton regime [26]. The recorded pulse trains possess the interval of 25 ns, corresponding to the fundamental repetition rate of 41.02 MHz.

Keeping pump power at 266.1 mW with an appropriate state of PC, and moving stage 2 along the horizontal direction only, the curvature of LPFG is increased from 0 to 2.199 m^{-1} . The relevant parameters are listed in Table 1. Continuous wavelength tuning range of 15.27 nm from 1582.02 to 1597.29 nm is then easily achieved, as shown in Fig. 2(a). Obviously, not only all spectra have Kelly sidebands, the shape of the solitons also hardly change, revealing that the pulses are almost stable. Figure 2(b) illustrates the variations of 3dB bandwidth and pulse width versus center wavelength. With the red shift of the center wavelength, the 3 dB bandwidth narrowed from 7.6 to 5.29 nm and the pulse width widened from 518.47 to 583.28 fs. We believe this is attributed to the depressed self-phase modulation (SPM) since the power decreases from 1.465 to 1.057 mW gradually. Moreover, the signal-noise ratio (SNR) at different center wavelengths is shown in Fig. 2(c). All SNRs are greater than 50 dB, manifesting good stability of the laser. Figure 2(d) shows a typical SNR at the center wavelength of 1582.02 nm.

In addition, the relationship between the center wavelength and the curvature of LPFG is exhibited in Fig. 2(e). They have a good linear correlation, implying that the tuning process is controllable. Yet, due to the limitation of the resolution of OSA and the precision of micrometer, the tuning coefficient reaches $0.22 \text{ nm}/0.033 \text{ m}^{-1}$ only. From Fig. 2(e), we can also see that the tuning process is highly reversible by changing the curvature of LPFG. We have repeated the procedure for a couple of more times, and the results persist.

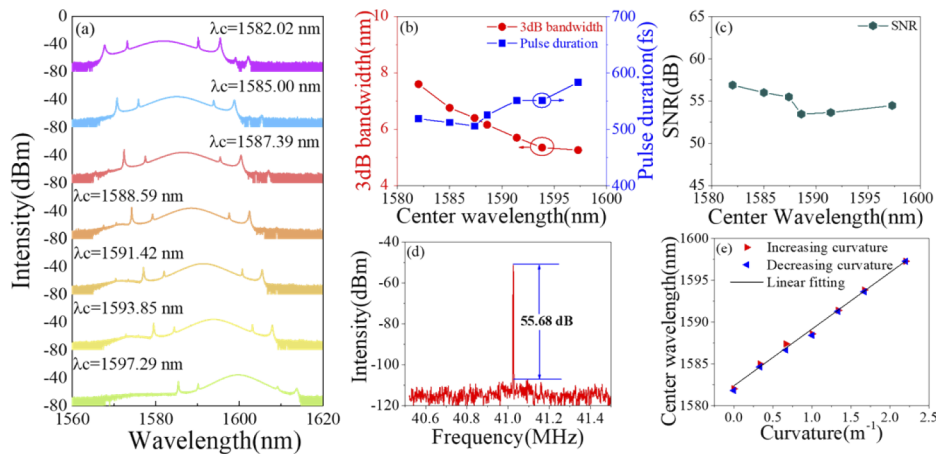


Fig. 2. (a) Tunable optical spectra at 266.1 mW pump power. (b) Variations of 3dB bandwidth and pulse duration versus center wavelength. (c) SNR at different wavelengths. (d) SNR at the wavelength of 1582.02 nm. (e) Center wavelength changes with the curvature of LPFG.

Table 1. Related parameters for the calculation of LPFG's curvature.

h (mm)	2a (mm)	1/R (m ⁻¹)
0	155	0
1	154.9	0.333
2	154.8	0.667
3	154.7	1.001
4	154.6	1.335
5	154.5	1.669
6.6	154.4	2.199

In our experiment, the output power varies from 1.465 to 1.057 mW, a total change of 0.408 mW within the continuous tuning range of 15.27 nm. This is mainly induced by the intrinsic gain unevenness. Compared with conventional VOAs, such variation of output power is small. Table 2 lists the output power change of the wavelength-tunable fiber lasers when using different VOAs. As referred in [17], using MA to control the cavity loss makes that the output power varies 0.118 mW when tuning the central wavelength of 1 nm approximately. Besides, using fiber taper as VOA also leads to output power change as high as 165 μ W/nm [23]. In comparison, LPFG-type NBOA in wavelength-tunable fiber laser has a relatively small impact on the output power, only 27 μ W/nm variation.

Table 2. Comparison of the influence of different VOAs on output power.

VOA	Tuning range (nm)	Variation of output power (mW)	Output power variation (μ W/nm)
MA [17]	46.7	~ 0.5-6.0	118
Fiber taper [23]	8.56	0.9-2.31	165
LPFG [this work]	15.27	1.465-1.057	27

Subsequently, we increase the pump power and adjust the PC. When the pump power exceeds the maximum energy that a pulse can withstand, a single pulse will be split into multiple pulses

due to the peak power limitation effect and energy quantization effect [27,28]. In our experiment, when the pump power is increased to 295 mW, 310.2 mW, 364 mW, 377.5 mW successively, the fiber laser operates at 2nd, 3rd, 4th, 5th harmonic mode locking (HML) with the repetition rates of 82.04 MHz, 121.4 MHz, 164.1 MHz, and 210.3 MHz. Considering the damage threshold of the SWCNTs used, we did not continue to increase the pump power.

Bending LPFG, wavelength tuning operation also could be achieved at 2nd to 5th HML. The tuning ranges are 14.11 nm, 14.78 nm, 13.71 nm, and 14.69 nm, respectively. Figure 3(a) shows the typical spectral tuning under 5th harmonic. The intensity of the spectrum is almost constant, while 3 dB bandwidth narrows at long wavelengths. The supermode suppression ratio (SMSR) [29] at different wavelengths is shown in Fig. 3(b), from which we can see that the SMSRs are generally greater than 30 dB. Note that the inset in Fig. 3(b) shows an example of the RF spectrum in 1 GHz span under 5th harmonic.

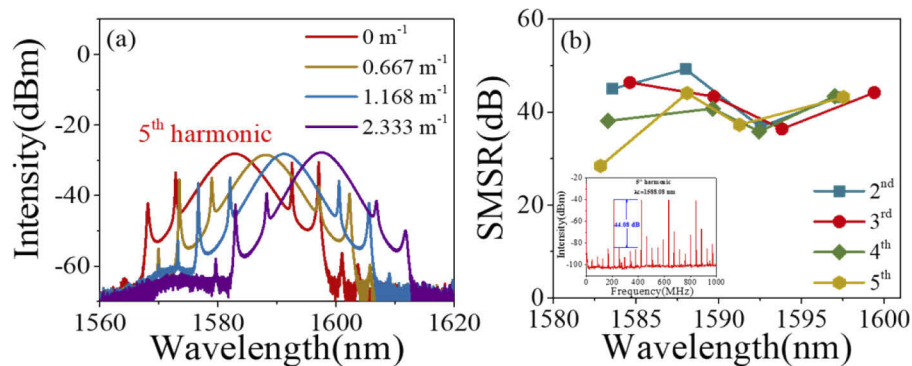


Fig. 3. (a) Tunable spectra of solitons at 5th harmonic. (b) SMSR at different wavelengths under HML.

To our understanding, the wavelength tuning operation based on LPFG can be explained as follows: The transmission spectrum of LPFG will be altered when it is bent. Thus, the wavelength and depth of interaction between loss induced by bending LPFG and gain within the emission bandwidth of the erbium ions is changed. With the modification of the net gain spectrum, the center wavelength of soliton is tuned [30–32]. Figure 4(a) depicts the transmission spectrum of the LPFG when increasing the curvature of LPFG from 0 to 2.199 m⁻¹. As the curvature of the LPFG increases, the rejection band red-shifts and its depth decreases gradually. The small signal gain of the EDF measured at the pump power of 222 mW is exhibited in Fig. 4(b). The reason for choosing this pump power is that the center wavelength is located at 1595.26 nm if the LPFG is replaced with SMF of the same length as shown in the inset in Fig. 4(b). Therefore, the net gain peak matches the mode locking wavelength when the pump power is fixed at 222 mW.

Figure 4(c) shows the product of the EDF gain and the LPFG transmission, which leads to the net gain spectrum of the ring cavity. The net gain peak locates at 1586.64 nm when the curvature of LPFG is 0 m⁻¹. Meanwhile, the central wavelength of the laser is located at 1582.02 nm. When the curvature of LPFG is increased to 0.333 m⁻¹, 0.667 m⁻¹, 1.001 m⁻¹, 1.335 m⁻¹, 1.669 m⁻¹, 2.199 m⁻¹ in successive by adjusting the displacement of stage 2, the net gain peak shifts to 1588.72 nm, 1589.20 nm, 1591.54 nm, 1596.64 nm, 1599.68 nm, 1600.28 nm. Similarly, the mode locking wavelength is tuned to 1585.00 nm, 1587.39 nm, 1588.59 nm, 1591.42 nm, 1593.85 nm, 1597.29 nm respectively. Figure 4(d) plots the tendency of net gain peak and mode locking wavelength versus the curvature of LPFG. We can see that the two have the same trend. However, due to the additional insertion loss of the SWCNTs, the mode locking wavelength is relatively shorter than net gain peak.

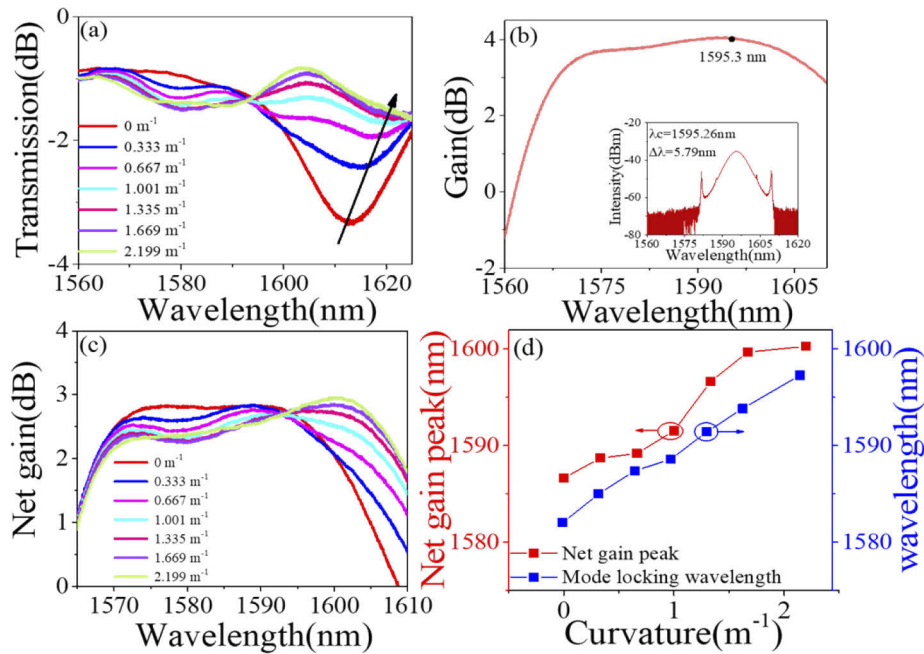


Fig. 4. (a) The change of the transmission spectrum when changing the curvature of LPFG from 0 to 2.199 m⁻¹. (b) Small signal gain spectrum. Inset, optical spectrum replaced LPFG with SMF of the same length. (c) Net gain spectrum. (d) The tendency of net gain peak and mode locking wavelength versus the curvature of LPFG.

Compared with conventional VOAs, this type of NBOA not only shows the effective gain shaping, but also has the advantage of less impact on output power. Figure 5(a) shows the tuning ranges from 1st to 5th HML. Single pulse has a wider tuning range since it is more stable than higher harmonics. However, there is no obvious relationship between harmonic orders and tuning range. Although the tuning range may be expanded under high pump power, higher harmonics generated from high pump power may be inherently unstable. Therefore, it may be difficult to achieve a wide tuning range under higher harmonics. Besides, the change of output power under different harmonic orders is exhibited in Fig. 5(b). We can see that with all available harmonics, the average output power changes $\sim 30 \mu\text{W}/1 \text{ nm}$, approximately 1/5 of the previously

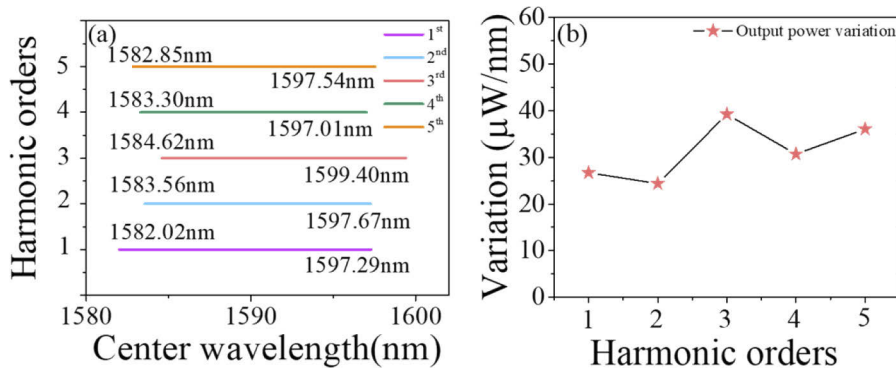


Fig. 5. (a) Tuning ranges, and (b) Output power variation under different harmonic orders.

reported references in [17,23], which indicates that LPFG-type NBOA has less effect on the output power vigorously. Moreover, our fiber laser has the shortest cavity length compared with those wavelength-tunable mode-locked fiber lasers demonstrated in previous, which improves the integration and compactness of the laser. However, in our experiment, when the curvature of the LPFG is further increased, a secondary rejection band will appear at the left of the principal rejection band. It is mainly caused by the coupling of the core and asymmetric cladding modes [33]. In our work, when the curvature of LPFG is bent from 0 to 2.199 m^{-1} , the contrast of the secondary rejection band is gradually increasing, but it is relatively low. Therefore, the secondary rejection band has no detrimental effect on the continuous tuning of our laser. If we further increase the curvature of the LPFG, due to the enhancement of the secondary rejection band, the central wavelength of the laser starts to blueshift. This is the primary cause for the limited tuning range. In the future, we will focus on optimizing the configuration of the length of EDF and characteristics of LPFG to achieve a wider tuning range.

4. Conclusions

In summary, we have demonstrated a L-band wavelength-tunable soliton mode-locked fiber laser, in which a single LPFG is functioned as a NBOA to realize the wavelength tuning operation. We have demonstrated that the wavelength tuning is achieved by modulating net gain profile. The LPFG-type NBOA based tunable mode-locked laser has advantages in lower output power variation and shorter cavity length than conventional VOAs. In this work, when increasing the curvature of LPFG from 0 to 2.199 m^{-1} , the central wavelength shifts from 1582.02 to 1597.29 nm (a total of 15.27 nm) under the pump power of 266.1 mW. The output power varies from 1.465 to 1.057 mW within the whole continuous tuning range, only a rate of $22\text{ }\mu\text{W/nm}$ variation. In particular, the tuning process is continuous, controllable and reversible. To our knowledge, this is the first time that LPFG is used as a NBOA to achieve center wavelength tuning with such lower power variation in a mode-locked fiber laser. The shortest cavity length of 5.08 m is also realized to obtain the wavelength-tunable mode-locked fiber laser. In addition, gradually increasing the pump power and adjusting PC, the laser can operate up to 5th HML. The associated tuning ranges are around 14 nm by bending LPFG. We would expect LPFG could serve as a novel type of nonlinear photonic device in ultrafast fiber lasers across a broad wavelength range.

Funding. National Key Research and Development Program of China (2020YFB1805800); National Natural Science Foundation of China (61605107, 61975107); Overseas Expertise Introduction Project for Discipline Innovation (D20031); Natural Science Foundation of Shanghai (20ZR1471500).

Disclosures. The authors declare that there are no conflicts of interest related to this article.

Data availability. Data underlying the results presented in this paper are not publicly available at this time but may be obtained from the authors upon reasonable request.

References

1. X. Hao, Z. Tong, W. Zhang, and Y. Cao, "A fiber laser temperature sensor based on SMF core-offset structure," *Opt. Commun.* **335**, 78–81 (2015).
2. Y. W. Lee and B. Lee, "Wavelength-switchable erbium-doped fiber ring laser using spectral polarization-dependent loss element," *IEEE Photonics Technol. Lett.* **15**(6), 795–797 (2003).
3. H. Zhang, D. Tang, R. J. Knize, L. Zhao, Q. Bao, and K. P. Loh, "Graphene mode locked, wavelength-tunable, dissipative soliton fiber laser," *Appl. Phys. Lett.* **96**, 111–112 (2010).
4. U. Keller, "Recent developments in compact ultrafast lasers," *Nature* **424**(2003).
5. N.-K. Chen, J.-W. Lin, F.-Z. Liu, and S.-K. Liaw, "Wavelength-Tunable Er³⁺-Doped fs Mode-Locked Fiber Laser Using Short-Pass Edge Filters," *IEEE Photonics Technol. Lett.* **22**(10), 700–702 (2010).
6. A. Mori, "Tellurite-Based Fibers and their Applications to Optical Communication Networks," *J. Ceram. Soc. Jpn.* **116**(1358), 1040–1051 (2008).
7. J. S. Harris, "Tunable Long-Wavelength Vertical-Cavity Lasers: The Engine of Next Generation Optical Networks," *IEEE J. Sel. Top. Quantum Electron.* **6**(6), 1145–1160 (2000).
8. F. Masaru, T. Yoshio, and O. Haruki, "Flat gain erbium-doped fiber amplifier in 1570nm-1600 nm region for dense WDM transmission system," in *Optical Fiber Communication Conference (OFCC)* (1997), paper PD3.

9. S. Huang, Y. Wang, P. Yan, J. Zhao, H. Li, and R. Lin, "Tunable and switchable multi-wavelength dissipative soliton generation in a graphene oxide mode-locked Yb-doped fiber laser," *Opt. Express* **22**(10), 11417–11426 (2014).
10. Y. Zhang, "C + L band wavelength and bandwidth tunable fiber laser incorporating carbon nanotubes," *Mod. Phys. Lett. B* **34**(30), 2050340 (2020).
11. Y. Yan, J. Wang, A. P. Zhang, Y. Shen, and H. Tam, "Tunable L-band Mode-Locked Bi-EDF Fiber Laser Based on Chirped Fiber Bragg Grating," in *Bragg Gratings, Photosensitivity, and Poling in Glass Waveguides (BGPP)* (2016), paper BM3B.5.
12. J. Wang, A. P. Zhang, Y. H. Shen, H. Y. Tam, and P. K. Wai, "Widely tunable mode-locked fiber laser using carbon nanotube and LPG W-shaped filter," *Opt. Lett.* **40**(18), 4329–4332 (2015).
13. J. Wang, M. Yao, C. Hu, A. Ping Zhang, Y. Shen, H. Y. Tam, and P. K. Wai, "Optofluidic tunable mode-locked fiber laser using a long-period grating integrated microfluidic chip," *Opt. Lett.* **42**(6), 1117–1120 (2017).
14. Q. Huang, C. Zou, C. Mou, X. Guo, Z. Yan, K. Zhou, and L. Zhang, "23 MHz widely wavelength-tunable L-band dissipative soliton from an all-fiber Er-doped laser," *Opt. Express* **27**(14), 20028–20036 (2019).
15. V. Deepa and R. Vijaya, "Effect of pump power on the tuning range of a filterless erbium-doped fiber ring laser," *Appl. Phys. B* **89**(2-3), 329–332 (2007).
16. G.-R. Lin and J.-Y. Chang, "Femtosecond mode-locked Erbium-doped fiber with intracavity loss controlled full L-band wavelength tunability," *Opt. Express* **15**(1), 97–103 (2007).
17. T. Zhu, Z. Wang, D. N. Wang, F. Yang, and L. Li, "Generation of wavelength-tunable and coherent dual-wavelength solitons in the C + L band by controlling the intracavity loss," *Photonics Res.* **7**(8), 853–861 (2019).
18. M. Melo, O. Frazão, A. L. J. Teixeira, L. A. Gomes, J. R. Ferreira da Rocha, and H. M. Salgado, "Tunable L-band erbium-doped fibre ring laser by means of induced cavity loss using a fibre taper," *Appl. Phys. B* **77**(1), 139–142 (2003).
19. H. Sakata, H. Yoshimi, and Y. Otake, "Wavelength tunability of L-band fiber ring lasers using mechanically induced long-period fiber gratings," *Opt. Commun.* **282**(6), 1179–1182 (2009).
20. G. Anzueto-Sánchez, A. Martínez-Rios, and J. Castellon-Urbe, "Tuning and wavelength switching erbium-doped fiber ring lasers by controlled bending in arc-induced long-period fiber gratings," *Opt. Fiber Technol.* **18**(6), 513–517 (2012).
21. S. Yin, R. Guo, M. Pérez Maciel, Y. López Dieguez, J. A. Montenegro Orenday, D. Jáuregui Vázquez, J. M. Sierra Hernández, E. H. Huerta Masscote, R. Rojas Laguna, and J. M. Estudillo Ayala, "A tunable wavelength erbium doped fiber ring laser based on mechanically induced long-period fiber gratings," in *Photonic Fiber and Crystal Devices: Advances in Materials and Innovations in Device Applications IX*, (2015).
22. S. Yin, R. Guo, M. Pérez Maciel, J. A. Montenegro Orenday, J. M. Estudillo Ayala, D. Jáuregui-Vázquez, J. M. Sierra-Hernandez, J. C. Hernandez-Garcia, and R. Rojas-Laguna, "Tunable wavelength erbium doped fiber linear cavity laser based on mechanically induced long-period fiber gratings," in *Photonic Fiber and Crystal Devices: Advances in Materials and Innovations in Device Applications X*, (2016).
23. L. Dai, C. Zou, Q. Huang, Z. Huang, Y. Ling, Z. Xing, Z. Yan, and C. Mou, "Continuously Tunable Mode-Locked Fiber Laser Based on Titled Fiber Grating," *Chinese Lasers* **46**(5), 0508026 (2019).
24. M. G. Xu, R. Maaskant, M. M. Ohn, and A. T. Alavie, "Independent tuning of cascaded long period fibre gratings for spectral shaping," *Electron. Lett.* **33**(22), 1893–1894 (1997).
25. T. Erdogan, "Cladding-mode resonances in short- and longperiod fiber grating filters," *J. Opt. Soc. Am. A* **14**(8), 1760–1773 (1997).
26. S. M. J. Kelly, "CHARACTERISTIC SIDEBAND INSTABILITY OF PERIODICALLY AMPLIFIED AVERAGE SOLITON," *Electron. Lett.* **28**(8), 806–807 (1992).
27. A. B. Grudinin, D. J. Richardson, and D. N. Payne, "ENERGY QUANTISATION IN FIGURE EIGHT FIBRE LASER," *Electron. Lett.* **28**(1), 67–68 (1992).
28. D. Y. Tang, L. M. Zhao, B. Zhao, and A. Q. Liu, "Mechanism of multisoliton formation and soliton energy quantization in passively mode-locked fiber lasers," *Phys. Rev. A: At., Mol., Opt. Phys.* **72**(4), 043816 (2005).
29. O. Pottiez, O. Deparis, R. Kiyon, M. Haelterman, P. Emplit, P. Mégret, and M. Blondel, "Supermode noise of harmonically mode-locked erbium fiber lasers with composite cavity," *IEEE J. Quantum Electron.* **38**(3), 252–259 (2002).
30. L. M. Åslund and S. D. Jackson, "Long-period grating as wavelength specific loss elements in fibre lasers," *Electron. Lett.* **43**(11), 614–615 (2007).
31. D. E. Ceballos-Herrera, I. Torres-Gomez, A. Martinez-Rios, G. Anzueto-Sanchez, and Y. Barmenkov, "Single- to three-wavelength switchable ytterbium-doped fiber laser based on intracavity induced loss by a long-period holey fiber grating," *Opt. Laser Technol.* **43**(4), 825–829 (2011).
32. P. Peterka, J. Maria, B. Dussardier, R. Slavík, P. Honzátko, and V. Kubeček, "Long-period fiber grating as wavelength selective element in double-clad Yb-doped fiber-ring lasers," *Laser Phys. Lett.* **6**(10), 732–736 (2009).
33. U. L. Block, V. Dangui, M. J. F. Dignonnet, and M. M. Fejer, "Origin of apparent resonance mode splitting in bent long-period fiber gratings," *J. Lightwave Technol.* **24**(2), 1027–1034 (2006).